Toward Understanding Extra-Large-Pore Zeolite Energetics and Topology: A Polyhedral Approach

Martijn A. Zwijnenburg, Stefan T. Bromley,* Jacobus C. Jansen, and Thomas Maschmeyer†

Laboratory of Applied Organic Chemistry and Catalysis, DelftChemTech, Delft University of Technology, Julianalaan 136, 2628 BL Delft, The Netherlands

Received March 8, 2003. Revised Manuscript Received July 3, 2003

Porous crystalline materials (e.g., zeolites, aluminophosphates) are widely used as catalysts, absorbents, and membranes. Two factors that largely determine the utility of any such material are its maximum pore/channel size and its energetic stability. Presently, the maximum pore size for materials stable enough to be of commercial use is approximately 8 Å. Extending the applicability of porous crystalline materials to encompass the control of molecules significantly larger than simple gases, and thus be of potential interest in the areas of fine-chemicals, pharmaceuticals, and nanotechnology, requires stable materials with larger pores. Unfortunately, no systematic, rational method exists to guide the development of such materials. Here, we show how for a large class of porous crystalline materials certain considerations of the topology and energetics of the constituent cages, using topological descriptors and quantum mechanical calculations, respectively, can lead to definite predictions regarding the stability of large pore/channel materials. The analysis formally demonstrates why smaller rings in such structures naturally compensate and help to stabilize large pores. These new insights allow us not only to predict the relative thermodynamic stability of a range of desirable (but as yet unmade) porous materials, but also to give practical advice to the experimentalist to guide their actual synthesis.

Introduction

Although great progress has been made in the application of zeolite-based catalysts and adsorbents in both the fine chemical and petrochemical industry, their use is limited to processes involving relatively small molecules.[1] This restriction is not due to any intrinsic chemical properties of existing zeolites, but simply to the fact that the pores of these zeolites are currently too small for many fine chemical substrates and heavier parts of petrochemical feedstock to enter. The desire to perform shape-selective adsorption and catalysis with molecules that are greater than 8 Å in size has fueled the demand for zeolites with extra-large pores (i.e., which contain rings circumscribed by more then 12 T-atoms[2]), and research into these materials has been pursued extensively in both industry and academia.[2−12] The search for such extra-large-pore materials, however, is hindered by the lack of a theoretical framework connecting the energetic stability of zeolites and their structure. Recent solution calorimetry experiments[13−15] have demonstrated that zeolites can become the thermodynamically preferred reaction product under synthesis conditions, i.e., in the presence of a template. Furthermore, for the calcined zeolite frameworks the measured entropic contributions are found to be an order of magnitude smaller than those of the corresponding enthalpic terms.[16,17] The entropic contribution also spans a considerably narrower range. Therefore, we believe that focusing on the framework energetics alone will still lead to useful results. We demonstrate that a better understanding of the link between zeolite structure and energetics can be obtained by decomposing zeolites into space-filling sets of face-sharing polyhedral units, leading to insights useful in the pursuit of extra-large pore zeolite syntheses.

* Corresponding author. Fax: +31-15-2784289. E-mail: S.T.Bromley@tnw.tudelft.nl.

† Current address: School of Chemistry, University of Sydney, Sydney, NSW, 2006, Australia.

(1) Davis, M. E. *Microporous Mesoporous Mater.* **1997**, *21*, 173.
(2) Davis, M. E. *Chem. Eur. J.* **1997**, *3*, 1745.
(3) Davis, M. E.; Saldarriaga, C.; Garces, J.; Crowder, C. *Nature* **1988**, *331*, 698.
(4) Estermanm, M.; McCusker, L. B., Baerlocher, C.; Merrouche, C, A.; Kessler, H. *Nature* **1991**, *352*, 320.
(5) Jones, R. H.; Thomas, J. M.; Chen, J.; Xu, R.; Huo, Q.; Li, S.; Ma, Z.; Chippindale, A. M. *J. Solid State Chem.* **1993**, *102*, 204.
(6) Balkus, K. J.; Gabrierlov, A. G.; Sandler, N. *Mater. Res. Soc. Symp. Proc.* **1995**, *368*, 369.
(7) Balkus, K. J.; Khanmamedova, A.; Gabrierlov, A. G.; Zones, S. I. *Stud. Surf. Sci. Catal.* **1996**, *101*, 1341.
(8) Lobo, R. F.; Tsapatsis, M.; Freyhardt, C. C.; Khodabandeh, S.; Wagner, P.; Chen, C. Y.; Balkus, K. J.; Zones, S. I.; Davis, M. E. *J. Am. Chem. Soc.* **1997**, *119*, 8474.
(9) Yoshikawa, M.; Wagner, P.; Lovallo, M.; Tsuji, K.; Takewaki, T.; Chen, C. Y.; Beck, L. W.; Jones, C.; Tsapatsis, M.; Zones, S. I.; Davis, M. E. *J. Phys. Chem B* **1998**, *102*, 7139.
(10) Li, H.; Laine, A.; O'Keeffe, M.; Yaghi, O. M. *Science* **1999**, *283*, 1145.
(11) Lee, G. S.; Nakagawa, Y.; Hwang, S. J.; Davis, M. E.; Wagner, P.; Beck, L.; Zones, S. I. *J. Am. Chem. Soc.* **2002**, *124*, 7024.
(12) Zheng, N.; Bu, X.; Wang, B.; Feng, P. *Science* **2002**, *298*, 2366.
(13) Petrovic, I.; Navrotsky, A. *Microporous Mater.* **1997**, *9*, 1.
(14) Piccione, P. M.; Yang, S.; Navrotsky, A.; Davis, M. E. *J. Phys. Chem B* **2002**, *106*, 3629.
(15) Yang, S.; Navrotsky, A. *Chem. Mater.* **2002**, *14*, 2803.
(16) Piccione, P. M.; Laberty, C.; Yang, S.; Camblor, M. A.; Navrotsky, A.; Davis, M. E. *J. Phys. Chem B* **2000**, *104*, 10001.
(17) Piccione, P. M.; Woodfield, B. F.; Navrotsky, A.; Davis, M. E. *J. Phys. Chem. B* **2000**, *104*, 10001.

10.1021/cm034132d CCC: $27.50
Published on Web 12/09/2003

To relate the single values of energy for each zeolite to the more diffuse concept of structure, it is desirable to have a simple calculable structure descriptor. Previous attempts to describe zeolite energetics focused on descriptors based on global structural data (framework density (FD), nonbonded distances, mean Si−O−Si angle[16,18,19]) relying extensively on geometry-optimized structures [to calculate framework densities, nonbonded distances and/or mean Si−O−Si angles, one needs accurate crystal data (obtainable only from (single)-crystal studies and/or energy minimizations), which makes them considerable difficult to calculate accurately] rather than the inherent topology of the framework. Furthermore, topologically independent concepts, such as framework density, are often not very intuitive when comparing and/or characterizing (novel) frameworks. For instance, LOV and MTN frameworks have comparable FDs (LOV FD = 18.3, MTN FD = 18.7) but completely different structures. The concept of a ring on the other hand is seemingly very intuitive and is often already used to characterize the pore-sizes in zeolites. However, due to the lack of a unique mathematical definition of a ring, ring statistics derived with different published methods[20−22] are often inconsistent.[22] Furthermore, these methods often find ring-sizes or numbers of rings that seem by inspection incorrect or too large. [The Crystana[20] algorithm for instance finds 12 rings in SOD and FER, which are not simply observed by inspection.]

Zeolites can also be described formally and intuitively as a space-filling packing of face-sharing polyhedra[23−25] and, thus, equivalently as tilings of Euclidian space with the polyhedra as tiles.[23,26,27] The latter fact has been used, for instance, in combinatorial tiling theory to systematically enumerate novel zeolite frameworks.[26−28] The faces of these polyhedra are, in contrast to rings, well-defined, and their geometrical properties (e.g., number of faces, total surface area, and average face size) are directly and uniquely related to the number of vertices by Euler's formula (eq 3a) [omitting T-atoms that are only two-connected after decomposition since they do not represent vertices of the polyhedron, but merely points at which an edge is bent]. In this study, rather than employing the concepts from polyhedral packing to classify and/or enumerate zeolites, we analyze the properties of the sets of polyhedra resulting from the space-filling decomposition of zeolites in order to gain insights into fundamental questions of zeolitic stability. An additional benefit of focusing on the properties of polyhedra is that combinatorial tiling methods often already output such sets of space-filling

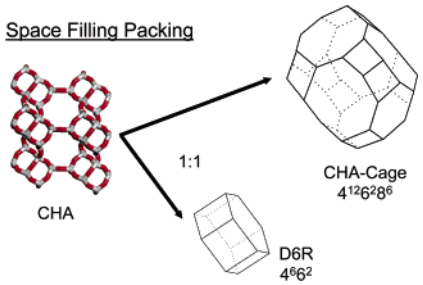

Figure 1. Decomposing zeolite CHA into a space filling set of polyhedra.

polyhedra into which a structure can be decomposed,[26−28] opening the possibility for high-speed analysis of structures obtained by enumeration. Furthermore, this "coarse-grained" description of zeolites opens the possibility of rationally designing new zeolites by combining different polyhedra into a space-filling packing. Figure 1 gives an example of the decomposition of a zeolite with the CHA framework.

On the basis of the above, we propose a new descriptor, which depends only on the underlying framework, i.e., using the polyhedra and their faces only. Our descriptor is given by two variables: the average and the variance of the face-size distribution of the polyhedra obtained from decomposing the zeolite, i.e., the first two cumelants. Furthermore, we demonstrate that these parameters are not only descriptive, but also predict which combinations of faces are needed to create the desired extra-large pores.

In this paper, we will limit ourselves to the correlation between energetics (binding energies) of such polyhedra and their face-size distribution. The rationale to first explore clusters rather then extended structures follows from the ease with which it is possible to generate such polyhedra and, thus, to extensively sample the various face-size distributions and their associated cumelants. We mainly focus on polyhedra in which all the vertices are three-connected. For the purpose of calculations, they are treated as silsesquioxanes ($H_nSi_nO_{1.5n}$). A significant percentage of all known zeolites can be decomposed in solely such polyhedra including among others SOD, LTA, FAU, RHO, KFI, DOH, AST, and CHA, the so-called simple tilings. To describe polyhedra in which some of the vertices are only two-connected (as appearing in frameworks as MFI, VFI, GIS and MOR and dense polymorphs such as quartz, cristabolite, and tridymite), a more extended version of theory is required which will be only touched upon presently and treated more elaborately in a later publication. Here, we study the energetics of bare silica cages, even though zeolites only become the thermodynamically preferred reaction-product in the presence of a template. However, experimental calorimetry[14] has shown the interaction enthalpy between template and framework to be small and to span only a narrow range of values consistent with the template/framework interaction being mainly due to weak dispersive forces. Furthermore, Gies and Marler concluded, in their work on the role of organic templates in the synthesis of clathrasils, that the chemical character of templates with similar shape had

(18) Petrovic, I.; Navrotsky, A.; Davis, M. E.; Zones, S. I. *Chem. Mater.* **1993**, *5*, 1805.
(19) Henson, N. J.; Cheetham, A. K.; Gale, J. D. *Chem. Mater.* **1994**, *6*, 1647.
(20) Goetzke, K.; Klein, H. J. *J. Non-Cryst. Solids* **1991**, *127*, 215.
(21) Hobbs, L. W.; Jesurum, C. E.; Pulim, V.; Berger, B. *Philos. Mag.* **1998**, *78* 679.
(22) Yuan, X.; Cormack, A. N. *Comput. Mater. Sci.* **2002**, *24*, 343.
(23) Wells, A. F.; Sharpe, R. R. *Acta Crystallogr.* **1963**, *16*, 857.
(24) O'Keefe, M.; Hyde, B. G. *Crystal Structures I: Patterns and Symmetry*; Mineralogical Society of America: Washington, DC, 1996.
(25) O'Keeffe, M. *Acta Crystallogr.* **1998**, *A54*, 320.
(26) Delgado Friedrichs, O.; Dress, A. W. M.; Huson, D. H.; Klinowski, J.; Mackay, A. L. *Nature* **1999**, *400*, 644.
(27) Delgado Friedrichs, O.; Huson, D. H. *Discrete Comput. Geom.* **2000**, *24*, 279.
(28) Foster, M. D.; Delgado Friedrichs, O.; Bell, R. G.; Almeida Paz, F. A.; Klinowski, J. *Angew. Chem., Int. Ed.* **2003**, *42*, 3896.

no influence on their templating ability.[29] This work is also in accordance with Monte Carlo docking calculations[30−32] that have demonstrated that for an organic molecule to template a zeolite successfully, the template must effectively fill the void space of the framework. It, thus, appears that a template molecule imposes its effective inverse shape on the framework by maximizing its interactions with the silica, thereby selecting a certain cage-type, but that this selectivity is not influenced by the specific nature and strength of the interactions alone. Although this paper focuses on zeolites, the general methodology developed herein is also applicable to other network materials as diverse as metallophosphates, silicon clathrates, fullerenes, and carbon nanotubes.

Computational Methodology

Silsesquioxanes and related silica clusters have been widely used as both experimental[33−37] and theoretical[38−45] model-systems for zeolites, due to their similarities with their periodic analogues in terms of structure and rigidity.[38] For these studies, ranging from investigations into the effect of ring-size and metal substitution on zeolite energetics to those focusing on vibrational modes of zeolites or on zeolite-based catalysis, the cluster approach with hydrogen termination was shown not to influence the outcome of these studies. From a theoretical point of view, hydrogen termination has been shown to be an efficient and accurate method for saturating the dangling bonds of the silica cluster,[46,47] owing much of its utility to the electronegativity of hydrogen lying between that of silicon and oxygen. For the purpose of calculations, we did not consider all of the possible isomers of all cages, but restricted ourselves to a combination of clusters found in zeolites, known isomers of silsesquioxanes and selected enumerated clusters. We explicitly decided to include non-zeolite-like clusters (for instance containing two membered silica rings not found in zeolites but present in other silica polymorphs[48,49]) to prevent biasing our results to known frameworks. Furthermore, we limited ourselves to clusters with a maximum of 24 T-atoms since accurate calculations on larger clusters would have been prohibitively demanding in terms of both computer-time and memory requirements. This choice of isomers allows for an optimal and efficient study of the effect of different face-size distributions on the stability of polyhedra.

All electron calculations were performed for 29 different silsesquioxanes employing density functional theory (DFT). The DFT calculations were performed using the three parameter B3LYP[50,51] functional and a 6-31G** basis set,[52,53] as implemented in the program Gaussian98.[54] This combination of functional and basis set has previously been successfully used by us[55] and other authors[44,56,57] for modeling similar silica systems. The geometric parameters for all clusters were fully optimized using the Berney algorithm[58,59] and tight optimization criteria (max force = 150^{-6} au, RMS force = 100^{-6} au, max displacement 60^{-6} au, RMS displacement 40^{-6} au). To ensure that true minima were found, all clusters were optimized without any symmetry constraints. Furthermore, for all clusters with less than 10 T-atoms, the use of symmetry in the wave function and gradient evaluation was explicitly disabled. Finally, it was verified that the symmetry for the converged clusters was equal or lower than that found in previous work.[38,43]

All energies reported for the silsesquioxanes are binding energies or binding energy differences normalized to the number of T-atoms in the polyhedron (kJ/mol/T-atom). Binding energies were calculated from the difference between the total energy of the silsesquioxane and the corresponding isolated singlet H and triplet O and Si atoms at the same level of theory. All silsesquioxanes are described as if they were 3-valent 3-connected polyhedra in which every Si−H group represents a vertex. Following Agaskar and Klemper,[60] we use the notation of X^n to represent n X-membered faces. For example, the double four-ring is given by 4^6, while a double six-ring will be represented as $4^6 6^2$ (see Figure 1).

Results

The binding energies calculated for all polyhedra and associated geometrical data are given in Table 1. An intriguing initial observation is that those polyhedra of this set, that have actually been found in zeolites, lie in a 3 kJ/mol/T-atom envelope above the lowest energy cage (see Figure 2). Second, it is noteworthy that within this region lie also two three-face containing polyhedra.

(29) Gies, H.; Marler, B. *Zeolites* **1992**, *12*, 42.
(30) Lewis, D. W.; Freeman, C. M.; Catlow, C. R. A. *J. Phys. Chem.* **1995**, *99*, 11194.
(31) Lewis, D. W.; Willcock, D. J.; Catlow, C. R. A.; Thomas, J. M.; Hutchings, G. J. *Nature* **1996**, *382*, 604.
(32) Lewis, D. W.; Sankar, G.; Wyles, J. K.; Thomas, J. M.; Catlow, C. R. A.; Willcock, D. J. *Angew. Chem., Int. Ed. Engl.* **1997**, *36*, 2675.
(33) Bornhauser, P.; Calzaferri, G. *J. Phys. Chem.* **1996**, *100*, 2035.
(34) Marcolli, C.; Lainé, P.; Bühler, R.; Calzaferri, G.; Tomkinson, J. *J. Phys. Chem. B* **1997**, *101*, 1171.
(35) Krijnen, S.; Harmsen, R. J.; Abbenhuis, C. L.; Van Hooff, J. H. C.; Van Santen, R. A. *Chem. Commun.* **1999**, 501.
(36) Duchateau, R.; Harmsen, R. J.; Abbenhuis, H. C. L.; Van Santen, R. A.; Meetsma, A.; Thiele, S. K.-H.; Kranenburg, M. *Chem. Eur. J.* **1999**, *5*, 3130.
(37) Liu, F.; John, K. D.; Scott, B. L.; Baker, R. T.; Ott, K. C.; Tumas, W. *Angew. Chem., Int. Ed.* **2000**, *39*, 3127.
(38) Earley, C. W. *J. Phys. Chem.* **1994**, *98*, 8693
(39) Hill, J. R.; Sauer, J. *J. Phys. Chem.* **1994**, *98*, 1238.
(40) Hill, J. R.; Sauer, J. *J. Phys. Chem.* **1995**, *99*, 9536.
(41) de Man, A. J. M.; Sauer, J. *J. Phys. Chem.* **1996**, *100*, 5025.
(42) Tossell, J. A. *J. Phys. Chem.* **1996**, *100*, 14828.
(43) Xiang, K. H.; Pandey, R.; Pernisz, U. C.; Freeman, C. *J. Phys. Chem. B* **1998**, *102*, 8704.
(44) Uzunova, E. L.; Nikolov, G. St. *J. Phys. Chem. A* **2000**, *104*, 5302.
(45) Kudo, T.; Gordon, M. S. *J. Phys. Chem. A* **2001**, *105*, 11276.
(46) Sauer, J. *Chem. Rev.* **1989**, *89*, 199.
(47) Kessi, A.; Delley, B. *Int. J. Quantum. Chem.* **1997**, *68*, 135.
(48) Weiss, A. *Z. Anorg. Allg. Chem.* **1954**, *276*, 95.
(49) Hamman, D. R. *Phys. Rev. B* **1997**, *55*, 14784.
(50) Becke, A. D. *J. Chem. Phys.* **1993**, *98*, 5648.
(51) Lee, C.; Yang, W.; Parr, R. G. *Phys. Rev. B* **1988**, *37*, 785.
(52) Binkly, J. S.; Pople, J. A.; Hehre, W. J. *J. Am. Chem. Soc.* **1980**, *102*, 939.
(53) Gordon, M. S.; Binkley, J. S.; Pople, J. A.; Pietro, W. J.; Hehre, W. J. *J. Am. Chem. Soc.* **1982**, *104*, 2797.
(54) Frisch, M. J.; Trucks, G. W.; Schlegel, H. B.; Scuseria, G. E.; Robb, M. A.; Cheeseman, J. R.; Zakrzewski, V. G.; Montgomery, J. A., Jr.; Stratmann, R. E.; Burant, J. C.; Dapprich, S.; Millam, J. M.; Daniels, A. D.; Kudin, K. N.; Strain, M. C.; Farkas, O.; Tomasi, J.; Barone, V.; Cossi, M.; Cammi, R.; Mennucci, B.; Pomelli, C.; Adamo, C.; Clifford, S.; Ochterski, J.; Petersson, G. A.; Ayala, P. Y.; Cui, Q.; Morokuma, K.; Malick, D. K.; Rabuck, A. D.; Raghavachari, K.; Foresman, J. B.; Cioslowski, J.; Ortiz, J. V.; Baboul, A. G.; Stefanov, B. B.; Liu, G.; Liashenko, A.; Piskorz, P.; Komaromi, I.; Gomperts, R.; Martin, R. L.; Fox, D. J.; Keith, T.; Al-Laham, M. A.; Peng, C. Y.; Nanayakkara, A.; Gonzalez, C.; Challacombe, M.; Gill, P. M. W.; Johnson, B. G.; Chen, W.; Wong, M. W.; Andres, J. L.; Head-Gordon, M.; Replogle E. S.; Pople, J. A. *Gaussian 98*, revison A.9; Gaussian, Inc.: Pittsburgh, PA, 1998.
(55) Zwijnenburg, M. A.; Bromley, S. T.; van Alsenoy, C.; Maschmeyer, T. *J. Phys. Chem. A* **2003**, *106*, 12376.
(56) Lopez, N.; Vitiello, M.; Illas, F.; Pacchioni, G. *J. Non-Cryst. Solids* **2000**, *271*, 56.
(57) Zhang, R. Q.; Chu, T. S.; Lee, S. T. *J. Chem. Phys.* **2001**, *114*, 5531.
(58) Peng. C.; Ayala, P. Y.; Schlegel, H. B.; Frisch, M. J. *J. Comput. Chem.* **1996**, *17*, 49.
(59) Peng, C.; Schlegel, H. B. *Isr. J. Chem.* **1994**, *33*, 449.
(60) Agaskar, P. A.; Klemperer, W. G. *Inorg. Chim. Acta* **1995**, *229*, 335.

Table 1. Face-Size Distribution, Average Face-Size, Standard Deviation (Square Root of the Variance), Binding Energy Normalized to the Number of Si Atoms (E_b), and Point Group of the Polyhedra[a]

N_v	face-size distribution	$\langle X \rangle$	σ_X	E_b (kJ/mol T-atom)	point group	remark
4	3^4	3.00	0.00	−1411.1	T_d	DFH-1
4	2^24^2	3.00	1.00	−1373.6	D_{2h}	
6	3^24^3	3.60	0.49	−1439.3	D_{3h}	DFH-2
6	$2^13^25^2$	3.60	1.20	−1417.2	C_{2v}	
6	2^36^2	3.60	1.96	−1382.2	D_{3h}	
8	4^6	4.00	0.00	−1448.8	O_h	DFH-3
8	$3^24^25^2$	4.00	0.82	−1444.4	C_{2v}	
8	3^46^2	4.00	1.41	−1434.5	D_{2h}	
8	2^48^2	4.00	2.83	−1383.6	C_s	
10	4^55^2	4.29	0.45	−1450.2	D_{5h}	
10	$3^14^35^3$	4.29	0.70	−1448.5	C_{3v}	
10	$2^14^46^2$	4.29	1.28	−1436.8	C_1	
12	4^55^4	4.50	0.50	−1450.7	D_{2d}	
12	4^66^2	4.50	0.87	−1449.7	D_{6h}	DFH-6
12	$3^14^45^16^2$	4.50	1.00	−1448.6	C_s	
12	3^25^6	4.50	0.87	−1448.1	D_{3d}	DFH-4
12	3^46^4	4.50	1.50	−1443.5	C_{3v}	DFH-5
14	4^35^6	4.67	0.47	−1450.0	D_{3h}	
14	$4^45^46^1$	4.67	0.67	−1450.7	C_{2v}	
14	4^66^3	4.67	0.94	−1450.1	D_{3h}	
14	4^77^2	4.67	1.25	−1449.1	D_{7h}	
14	$3^24^58^2$	4.67	1.83	−1445.1	C_{2v}	
16	4^25^8	4.80	0.40	−1451.2	C_2	DFH-12
16	$4^45^46^2$	4.80	0.75	−1450.8	C_{2h}	DFH-9
16	4^66^4	4.80	0.98	−1450.2	C_s	DFH-10
16	4^88^2	4.80	1.60	−1448.4	D_{8h}	DFH-8
18	4^66^5	4.91	1.00	−1450.1	C_{2v}	DFH-17
20	5^{12}	5.00	0.00	−1451.2	D_2	
24	4^66^8	5.14	0.99	−1449.7	O_h	DFH-27

[a] DFH-N corresponds to polytope N, as defined by Delgado-Friedrichs and Huson.[27]

The average face size of a polyhedron can be calculated from the face size distribution of a polyhedron via

$$\langle x \rangle = \frac{\sum_{i=1}^{N_f} x_i}{N_f} \tag{1}$$

Here, N_f is the total number of faces and x_i the face size of the ith face of the polyhedron. Furthermore, one can define the number of vertices of a polyhedron, N_v, in terms of the constituent faces via

$$N_v = \frac{1}{3}\sum_{i=1}^{N_f} x_i \tag{2}$$

While N_f can be expressed as a function of the number of vertices by applying Euler's equation and by realizing that the stoichiometry of those polyhedra, those that contain three connected vertices exclusively fix the ratio between vertexes and edges as 1:3

$$N_v + N_f - N_e = 2 \tag{3a}$$

$$N_f = 2 + \frac{1}{2}N_v \tag{3b}$$

Substitution of the latter two results in equation 1 gives the formula for the average face size of a polyhedron:

$$\langle x \rangle = \frac{3N_v}{2 + \frac{1}{2N_v}} \tag{4}$$

The average face size, thus, only depends on the number of vertices (T-atoms) of a polyhedron and is, therefore, equal for all isomers.

Figure 2 shows how the binding energies of the polyhedra vary with the average face size. While it clearly shows the effect of isomers, i.e., multiple energy values for one average face size, it also shows a correlation between the lowest energy isomers and their corresponding average face sizes. Average face size thus, as to be expected from the fact that it is equal for isomers, only describes part of the energetics of the polyhedra. Furthermore, the graph shows an effective upper boundary to the binding energy of three connected polyhedra given by polyhedra of a ($2^{n/2}n^2$) nature.

The second cumulant (variance) can be calculated from the face size distribution of a polyhedron via

$$\sigma_X{}^2 = \frac{\sum_{i=1}^{N_f}(X_i - \langle X \rangle)^2}{N_f} \tag{5}$$

Figure 3 shows how the binding energy of isomeric polyhedra changes with their associated variance. [For ease of visualization, we plot the standard deviation rather than the variance. The standard deviation equals the square root of the variance.] For each set of isomers, one can observe a strong and closely similar correlation between binding energy and the variance of their face-size distribution. Furthermore, the slope of the correlation consistently decreases with increasing average face size. Both observations are consistent with the energetics of three-connected polyhedra being described by a surface defined in terms of the average and variance of the face-size distribution. One point of interest can be observed in Figure 3b for an average face size of 4.5, where there are two cages ((3^25^6) and (4^66^2)) with the same variance but different binding energies. In such rare cases, when two polyhedra have equal average and variance but a different face-size distribution, our two-parameter description is inherently not sufficient to distinguish between their energies.

Discussion

The energetics of the polyhedra can be described in terms of the average and the variance of their face-size distribution. However, for these descriptors to have any more value than merely statistical, one has to understand their physical significance. It is known from previous calculations that smaller rings are more strained than larger rings and that their binding energy is inversely proportional to a function of their ring size.[61,62] It should, therefore, be expected that if the average face-size would be a complete description of the system, the

(61) Kudo, T.; Nagase, S. *J. Am. Chem. Soc.* **1985**, *107*, 2589.
(62) Kramer, G. J.; de Man, A. J. M.; van Santen, R. A. *J. Am. Chem. Soc.* **1991**, *113*, 6435.

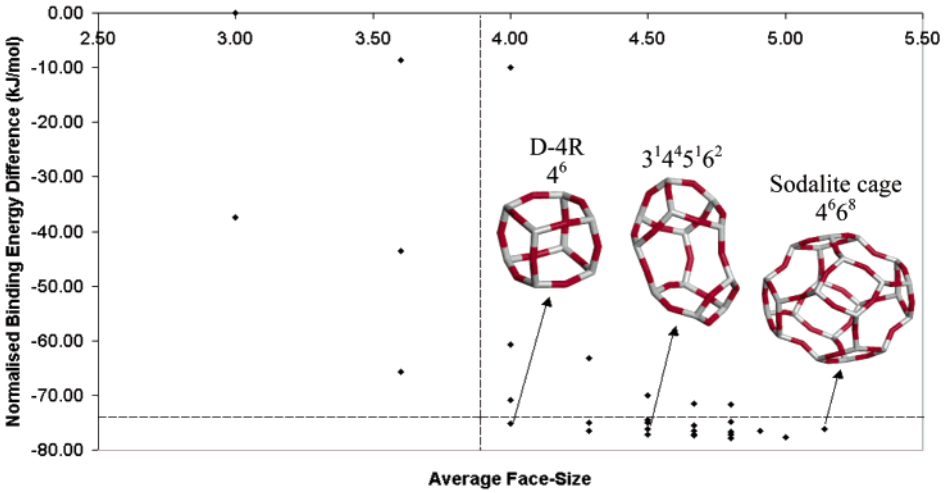

Figure 2. Calculated binding energies (normalized to the number of Si atoms) versus the average face-size of the polyhedra (box as discussed in text). The terminating hydrogen atoms are omitted for ease of visualization.

energy would also vary with inverse proportionality to the average face-size. This trend is indeed clearly recovered for the cages when considering only the lowest energy cages for each average ring size (see Figure 4). To these special cages we will refer hereafter as "principal polyhedra". It is interesting to note that the larger principle polyhedra ($\langle X \rangle \geq 4$) are all commonly found in clathrasils.[29] Principal polyhedra are found to be those cages consisting of either only one face-size (if the average face size is integral) or of those solely consisting of the two types of faces closest to the average face size. Thus, by definition, principal polyhedra are the polyhedra with minimal variance for each set of isomers. To investigate this further, a model of how the energies of cages vary with the different faces possibly present has been developed. A first approximation, neglecting everything but the energies, E_i's, of the individual faces (normalized to the number of T-atoms in the face, kJ/mol/T-atom), results in the following expression for the cage energy:

$$E_{\text{cluster}} = \frac{1}{3N_{\text{v}}} \sum_{i=1}^{N_{\text{f}}} x_i E_i \qquad (6)$$

Assuming that E_i is a well-behaved function of the face-size, E_i can be expressed in terms of a power series in x_i:

$$E_i = \alpha_0 + \frac{\alpha_1}{x_i} + \frac{\alpha_2}{x_i^2} + \ldots \qquad (7)$$

Substitution of eq 7 in eq 6 results in

$$E_{\text{cluster}} = \frac{1}{3N_{\text{v}}} \sum_{i=1}^{N_{\text{f}}} \left(\alpha_0 x_i + \alpha_1 + \frac{\alpha_2}{x_i} + \ldots \right) \qquad (8)$$

By applying eq 2 to the first term in the summation, this can be written, in turn, as

$$E_{\text{cluster}} = \alpha_0 + \frac{\alpha_1}{\langle X \rangle} + \frac{1}{3N_{\text{v}}} \sum_{i=1}^{N_{\text{f}}} \left(\frac{\alpha_2}{x_i} + \ldots \right) \qquad (9)$$

While this expression is only an approximation and while we have no knowledge about the precise magnitude of the coefficients, it clearly shows that energy should vary with inverse proportionality to the size of the face and linearly with is occurrence as long as E_i decreases monotonically and has a horizontal asymptote. The principal polyhedra now should be the isomers, which minimize the cage energy (eq 9) within the boundary conditions imposed by eq 3b. While such a minimization is far from facile due to the general nature of the energy function, it is possible to study, by inspection, the correlation between binding energy and variance. Increasing the variance corresponds to replacing faces close to the average face-size with both smaller and larger faces, while keeping the total number of faces constant as required by Euler's equation (eq 3b). Therefore, upon increasing the variance of a polyhedron, the face-size distribution becomes broader and more asymmetric, resulting in more and more faces being smaller than the average face-size and fewer and fewer faces being larger than the average. The combination of the latter with the fact that, according to the form of eq 9, smaller faces raise the energy of a polyhedron considerably (while larger faces only slightly decrease the energy) provides an explanation for the observed positive correlation between the variance and binding energy of isomers. Minimization of the cage energy for a certain polyhedron size, N_{v}, corresponds to a minimization of the variance, while keeping the average face-size constant. The principal polyhedra are, therefore, as observed, those polyhedra with minimal variance for each set of isomers.

In the same way as the principal polyhedra were shown to be the isomers with minimal variance, the effective upper boundary of binding energies can be defined by polyhedra which maximize the variance. Although again no formal proof will be given, one can easily see that for $N_{\text{v}} = n$ an isomer of ring-like nature ($2^{n/2}n^2$) will have the highest variance obtainable for that polyhedron. All the binding energies of three-connected polyhedra, thus, lie in an envelope (not shown), with the energies of the ($2^{n/2}n^2$) isomers as upper boundary and the energies of the principal polyhedra as lower boundary. Summarizing, the energy of polyhedra can be described as a surface defined by the average and variance of the face-size distribution, with the line

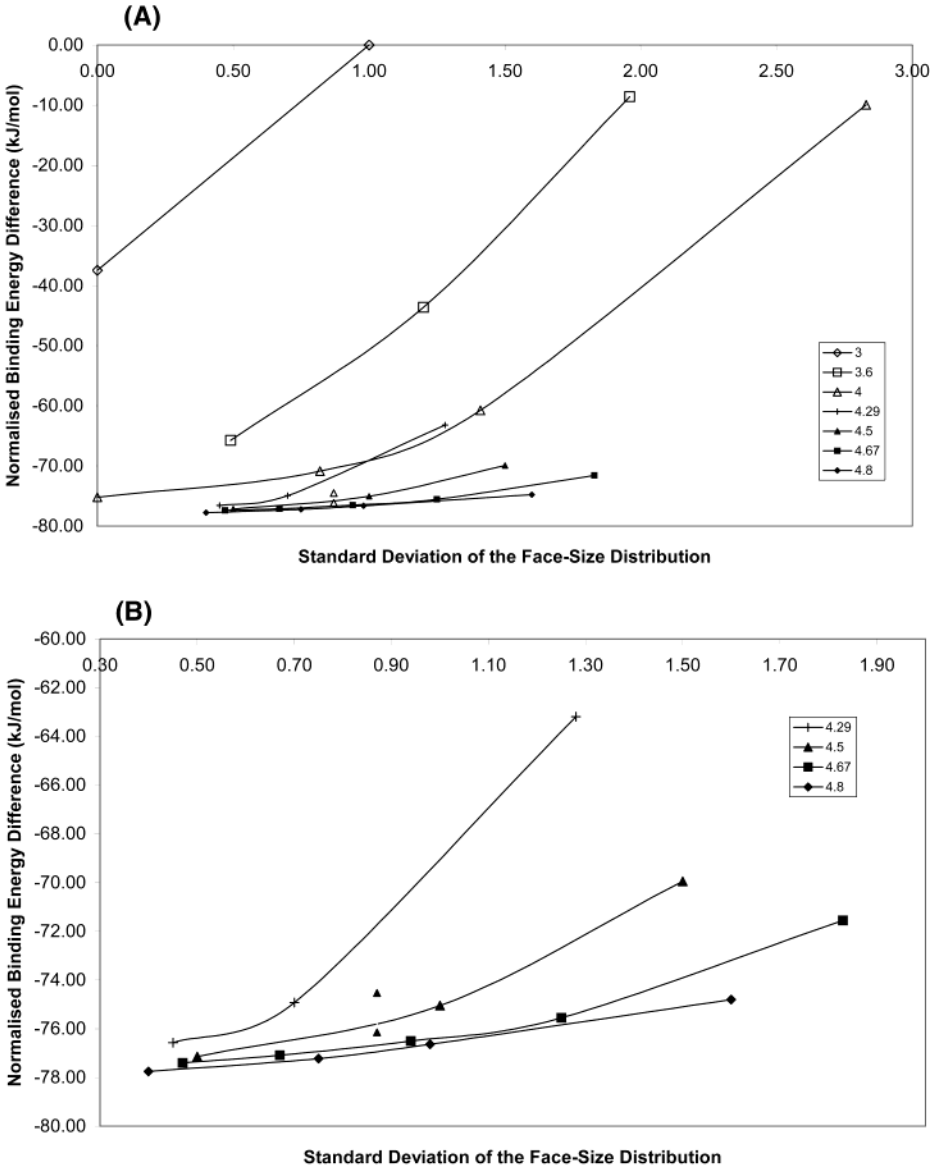

Figure 3. (A) Calculated binding energies (normalized to the number of Si atoms) versus the standard deviation (square root of the variance) of the face-size distribution for the various sets of isomers. The lines are guides to the eyes. (B) Calculated binding energies (normalized to the number of Si atoms) versus the standard deviation (square root of the variance) of the face-size distribution for the various sets of isomers (magnification of Figure 3A). The lines are guides to the eyes.

connecting the principal polyhedra as limits for minimal variance and the line connecting the ($2^{n/2}n^2$) polyhedra as limit for the maximal variance.

The results discussed above for three-connected polyhedra, and thus silsesquioxanes, now can be expanded to understand zeolites. As discussed in the Introduction, there exists a significant portion of zeolites which can be fully decomposed into solely three-connected polyhedra. For such zeolites, the polyhedra would be expected to be more than only model systems, and the correlations obtained for the polyhedra would be expected to also hold for these zeolites. When expressing the energetic stability of such zeolites as their transition enthalpy to quartz,[16,18] we should therefore expect a decreasing transition enthalpy with the average face size and an increasing transition enthalpy with increasing variance of the face-size distribution. Preliminary calculations have shown that this is indeed the case for a large subset of structures (more extensive results will be published separately). Moreover, due to the generality of the derivation (eqs 6−9), which make no reference to the specific chemical constitution of the polyhedra involved, we expect our predicted correlations to hold also for substituted zeolites, and metallophosphates.

Before investigating the problem of zeolite stability in general, it is worth focusing upon the energetics of polyhedra with three-faces as it has been suggested in the past that zeolites containing such cages are especially disadvantageous.[38] This assumption is supported by the fact that no three-face-containing zeolite framework has, thus far, been crystallized in the all-silica form and that three-face containing zeolites mostly contain special T-atoms (Be, Li, Zn). Our results, in contrast, indicate that the presence of small faces is not, by definition, as detrimental to the energetic stability of zeolites as previously thought. The presence of three-faces, indeed, increases the energy compared to larger faces, but the size of this destabilization critically depends on the concentration of such faces. Two of our three-face-containing polyhedra lie within 3 kJ/mol/T-

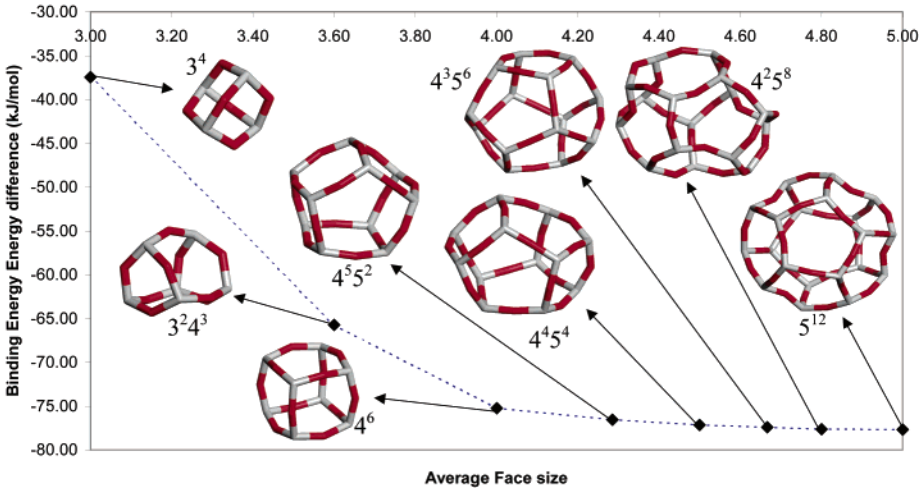

Figure 4. Calculated binding energies (normalized to the number of Si atoms) versus the average face-size of the principal polyhedra. The terminating hydrogen atoms are omitted for ease of visualization.

atom of the lowest energy polyhedron, just slightly above the cube ("double four ring D-4R"). These results are of special interest since one of these cages is the three-face containing cage found in ZSM-18 (MEI framework). The reason other authors[38] found that three-face-containing structures were significantly less stable than those only containing larger faces is that only very small silsesquioxanes (e.g., tetrahedron) were studied, all of which possess high three-face concentrations. Three-face-containing zeolites are, thus, very likely to be more stable than previously expected.

Generally, our conceptual approach can further explain some important characteristics of zeolites decomposable in solely three-connected polyhedra. Since the pores/channels in zeolites are an integral part of the crystal structure, the rings controlling the diffusion through the channels should equal the faces of the constituting polyhedra. A zeolite with 8- and 12-ring channels should therefore, for example, consist of polyhedra with faces of 8 and 12 Si-atoms (although these do not necessarily have to be in the same polyhedron). [Rings smaller than 8 Si atoms are commonly not seen as part of channels because they are assumed to be too small for molecular diffusion (although diffusion of He, H_2, and H_2O occurs through 6-rings) and only part of the faces of a polygon will thus be part of a channel.] The average face size of a three-connected polyhedron, however, has a limit of six: as can be seen from rewriting eq 4 as a constant and a term that vanishes as N_v tends to infinity.

$$\langle x \rangle = 6 - \frac{6}{1 + \frac{N_V}{4}} \qquad (10)$$

This is in-line with the average ring (face) size of polyhedra decomposable four-connected nets, as derived by O'Keefe et al. (eq A3.15 in ref 24).

A three-connected polyhedron with faces larger than five should, therefore, always have faces smaller than six to compensate. Starting from a "dense" [principal polyhedra always have only faces of six or smaller and a principal polyhedra can therefore never be part of a channel in a structure (see above)] structure, consisting of principal polyhedra, creating and subsequently increasing the size of channels corresponds to increasing the variance, and thus to decreasing the energetic stability of the constituent polyhedra. The extra energetic cost of larger pores can be compensated somewhat by increasing the size of polyhedra the zeolite consists of, thereby increasing the average face-size (the other energy-dependent parameter of our descriptor), provided the number of vertices is far from the limit. This effect can be observed when comparing the 8 Si-atom ($3^24^25^2$) and the 24 Si-atom (4^66^8) cages: while the larger cage has eight 6-faces, larger than any face in the smaller cage, and, furthermore, has a less energetically favorable variance than the smaller cage, it is 5.3 kJ/mol/T-atom lower in energy than the smaller cage due to its larger average face size. While this effect appears to become negligible at average face-sizes larger than 4.8, where the energy difference between cages with similar variance is insignificant (<0.1 kJ/mol, see for example the flattening of trend shown in Figure 4), large cages are still an energetically favorable means to incorporate large pores. This is simply due to the fact that cages with an increased size, and therefore more vertices, allow for face sizes closer to the limiting value of 6 to be used for compensation for the introduction of large pores (e.g., many five-faces instead of few three-faces) thereby lowering the variance, and thus the energy. Normally, zeolites consist of a mixture of different polyhedra. The inclusion of low variance (principal) polyhedra lowers the energy of the framework [under the reasonable assumption that $E_{zeolite} \propto \sum E_{polygon}$] by diluting the energetic disadvantage of the higher variance polyhedra. The resulting zeolite, however, will always be higher in energy than a zeolite solely consisting of low variance (principal) polyhedra.

On the basis of the above, one can now calculate the minimum cage-sizes (three-connected polyhedra) needed to accommodate certain types of catalytically interesting channel-systems, when assuming that they only contain the desired faces (corresponding to extra-large pores) and compensating three-, four-, or five-faces. The results of these calculations for several (extra-) large channel systems (12***, 14***, 18***, 14**, 18**, 14*, 18*, where the number of asterisks denotes the dimensionality of the pore system) can be found in Table 2. The first thing to note is, since the energy of these large poly-

Table 2. Face-Size Distribution, Number of Vertices, Average Face-Size, and Standard Deviation (Square Root of the Variance) of the Minimum Cages Needed to Accommodate Five Catalytically Interesting Channel-Systems in Order of Increasing Variance[a]

channel system	face-size distribution	N_v	$\langle X \rangle$	σ_X^2
12***	$5^{48}12^6$	104	5.78	2.20
14*	$5^{28}14^2$	56	5.6	2.24
14**	$5^{44}14^4$	92	5.75	2.49
14***	$5^{60}14^6$	128	5.82	2.59
18*	$5^{36}18^2$	72	5.68	2.90
18**	$5^{60}18^4$	124	5.81	2.18
12***	$4^{24}12^6$	56	5.60	3.20
18***	$5^{84}18^6$	176	5.87	3.24
14*	$4^{14}14^2$	28	5.25	3.31
14**	$4^{22}14^4$	48	5.54	3.61
14***	$4^{30}14^6$	68	5.67	3.73
12***	$3^{16}12^6$	40	5.45	4.01
18*	$4^{18}18^2$	36	5.40	4.20
18**	$4^{30}18^4$	64	5.65	4.51
18***	$4^{42}18^6$	92	5.75	4.63
14***	$3^{20}14^6$	48	5.54	4.63
18*	$3^{12}18^6$	24	5.14	7.07
18**	$3^{20}18^4$	44	5.50	5.59
18***	$3^{28}18^6$	64	5.65	5.72

[a] The number of asterisks indicates the dimensionality of the pore system.

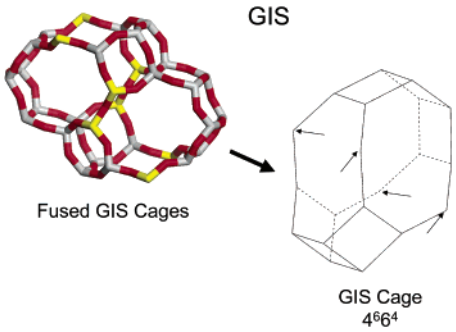

Figure 5. Decomposing zeolite GIS into a space filling set of polyhedra (2-connected vertices highlighted).

hedra is described by only the variance of their face-size distribution (see above) and their energetic stability is inversely proportional to a function of this variance, the ordering of the energetic stability of the channel-systems for the same pore-size is predicted to go as one-dimensional (2 extra-large faces) > two-dimensional (4 extra-large faces) > three-dimensional (6 extra-large faces). Furthermore, using the same argument the energetic ordering of channel-systems is predicted to be as 12 > 14 > 18. From an energetic point of view, we would, therefore, expect that the probability of synthesizing extra-large-pore zeolites decreases with both the dimensionality of its channel-system and the size of the pores. The data in Table 2 also show that, as explained above, for the same channel-system dimensionality and pore-size, the variance can be lowered by increasing the size of compensating faces. The lowest variance polyhedra from Table 2 are all larger than 56 vertices, while the largest polyhedra currently known in synthetic zeolites have 48 vertices [LTA, RHO, KFI, $4^{12}6^8 8^6$; FAU, $4^{18}6^4 12^4$]. A natural zeolite containing a 96 vertex cage is known (TSC, $4^{24}6^8 8^{18}$), but this cage contains a nonremovable Cu^{2+}_{48} $(OH)^-_{128}$ cluster.[63] Synthesizing zeolites with such large cages poses a significant synthetic challenge. Furthermore, upon increasing the size of the compensating faces, clathrasil cages containing only 5- and 6-faces become quickly more stable than the higher-variance large-faced cages, further decreasing the chance of a successful synthesis of the large-faced cages.

For zeolites that can be decomposed in polyhedra containing both two and three connected vertices (mixed-vertex polyhedra), the situation is somewhat more complicated. While upon adding two-connected vertices to a polyhedron the number of faces remains constant, the face-size of the faces in which the vertices are inserted increases. Taking λ to equal the ratio between two and three connected vertices (for example GIS: $N_{v2} = 4$, $N_{v3} = 16$, $\lambda = 4/16$, see Figure 5) of a polyhedron, the average face size equals

$$\langle x \rangle = \frac{(3 + 2\lambda)N_{v3}}{2 + \frac{1}{2}N_{v3}} \qquad (11)$$

This, in turn, can be written in a way analogous to eq 10:

$$\langle x \rangle = 6 + 4\lambda - \frac{6 + 4\lambda}{1 + \frac{N_{v3}}{4}} \qquad (12)$$

The average face size of mixed-vertex polyhedra, thus, has a limit of $6 + 4\lambda$ as N_{v3} tends to infinity and only faces larger than $5 + 4\lambda$ need compensating by smaller faces. The fact that the average face size increases with increasing λ suggests that increasing λ might be an alternative route to extra-large pores. Preliminary calculations suggest that polyhedra with $\lambda \neq 0$ are slightly more energetically stable than their $\lambda = 0$ analogues. This is an observation that is supported by experimental calorimetric measurements[16,18] where all low-lying silica polymorphs are those (partly) decomposable into mixed-vertex polyhedra. The data in Table 2 are calculated for three-connected polyhedra ($\lambda = 0$). To calculate the equivalent of Table 2 for polyhedra with $\lambda \neq 0$ would be a formidable task because of the extra degree of freedom. It is evident, however, that, when allowing λ to change freely, one can accommodate channel-systems in much smaller cages than when $\lambda = 0$ (even with a lower variance). This is clearly illustrated by the 12^6 ($\lambda = 3$) cage found in zeolite ITQ-21.[64]

Applying our conceptual methodology to the prediction and rationalization of actual experimental all-silica syntheses is complicated by many factors. However, from cage energetics alone, one would expect (at least for $\lambda = 0$ zeolites) the formation of frameworks containing many principal polyhedra, i.e., clathrasil-like structures. Clathrasils are, indeed, often found as product in SiO_2/template/H_2O systems,[29] e.g., AST, DOH, MEP, MTN, SOD (all $\lambda = 0$). However, besides such materials, a range of larger-faced porous all-silica structures, for example the $\lambda = 0$ materials, chabazite (CHA), decadodecasil 3R (DDR), SSZ-23 (STT), RUB-3 (RTE), and the $\lambda \neq 0$ materials, beta (BEA), ITQ-4 (IFR), SSZ-24

(63) Effenberger, H.; Giester, G.; Krause, W.; Bernhardt, H. J. *Am. Mineral.* **1998**, *83*, 607−617.

(64) Corma, A.; Diaz-Cabanas, M. J.; Martinez-Triguero, J.; Rey, F.; Rius, J. *Nature* **2002**, *418*, 514.

(AFI), CIT-5 (CFI), have also been synthesized successfully.[29,65,66] The formation of these larger-faced structures, at first sight, appears to be in contradiction with the results of our calculations. However, on closer examination this issue can be resolved by considering further the role of the template. Molecules with a small aspect ratio, like small cyclic molecules, while rotating effectively fill the lowest-energy cages (principal polyhedra). Template molecules with a large aspect ratio, such as linear or branched molecules, do not fill, or even fit into, these cages. Such large aspect ratio templates seem to force their structure upon the cages, resulting in cages other than principal polyhedra, but possibly with the desired larger faces. Such a model of the influence of template molecule is in line with the experimental observation of Gies and Marler that while clathrasils are the exclusive product when the template is a small mono-, bi-, or tricyclic molecule, upon changing the template to a linear or branched molecule, the products display tubular structures.[29] A similar change of structural characteristics has also been observed by Nakagawa et al.[67] upon increasing the size of their bridged bicyclic template molecule. We, thus, speculate that siliceous zeolite cages with the desired large or extra-large faces are necessarily nonspherical and can only be synthesized from template molecules having a high aspect ratio. An experimental illustration of this prediction is that the small aspect ratio *tert*-butyltrimethylammonium cation templates the $4^6 6^{12}$ cage in AST,[68] while the higher aspect ratio *N,N,N*-trimethyladamantammonium cation templates the $4^{12} 6^2 8^6$ cage of CHA.[69] Thus the fact that using the 18-crown-6 complex of sodium as template in the synthesis of the non-all-silica zeolite MCM-61[70] (MSO framework) results in the formation of large clathrasil cages ($4^6 6^{20}$) rather than the desired large-faced cages can also most likely be explained by the small aspect ratio of the template employed. Whether this observation holds for zeolites generally is a more complex question, since metal substitution may change the relation between a cage-type (face-size distribution) and its energetic stability, and thus perhaps preferably stabilize large-faced cages, in line with observations by Corma et al. for germanium substituted frameworks.[71]

On the basis of the above, we can conclude that synthesizing extra-large-pore zeolites corresponds, at least for zeolites decomposable in $\lambda = 0$ polyhedra, to steering the synthesis mixture toward a combination of small rings and large cages, probably via the use of large aspect ratio templates. The presence of sufficient small rings herein is critical since otherwise the more energetically stable polyhedra, with predominantly five- and six-faces, will be formed most probably, resulting in clathrasils rather than extra-large-pore zeolites. Therefore, additives that promote the formation of a certain number of 3-rings may point the way toward large-pore zeolites. For zeolites decomposable into $\lambda \neq 0$ polyhedra, the situation is considerably less clear. However, on the basis of the results achieved so far, we feel confident that eventually for all zeolites the presence of extra-large-pores can be coupled to properties of their constituting polyhedra and that more general rules regarding the synthesis of extra-large-pore zeolites will be derived.

Conclusions

Synthesising extra-large-pore zeolites appears, thus, to be all about striking a fine balance between face- and cage-sizes with the energetic stability of large-faced cages depending predominantly on the variance of the face-size distribution. Our investigation has shown that decomposing zeolites into polyhedra combined with Euler's rule and DFT calculations can give remarkable insights into the fundamental properties of zeolites. In particular, we have shown that the energetic destabilization of zeolites by small rings depends on their concentration and can be as small as only 2.6 kJ/mol. We further demonstrate that the energetics of three-connected polyhedra, as modeled by silsesquioxanes, can be understood in terms of a two parameter descriptor utilizing both the average and variance of their face-size distribution, and propose that the same correlations should hold for all zeolites which can be thought of as completely decomposable into three-connected polyhedra. For the same class of zeolites we have formally established that large pores require compensation by small faces and that the more energetically stable, extra-large pore zeolites are the ones consisting of large polyhedra. Finally, we demonstrate that steering the synthesis mixture toward small rings and large cages most likely offers a route to extra-large-pore zeolites.

Acknowledgment. This work was sponsored by the stichting Nationale Computerfaciliteiten (National Computing Facilities Foundation, NCF) regarding the use of supercomputer facilities, with financial support from the Nederlandse Organisatie voor Wetenschappelijk Onderzoek (Netherlands Organization for Scientific Research, NWO). We thank Drs. M.D. Foster, R.G. Bell, A. Simperler, E. Flikkema, and H. van Koningsveld for useful discussions and Dr. J. C. Wojdel for help with the figure graphics.

CM034132D

(65) Marler, B.; Grünewald-Lüke, A.; Gies, H. *Zeolites* **1995**, *15*, 388.
(66) Camblor, M. A.; Villaescusa, L. A.; Diaz-Cabañas, M. J. *Top. Catal.* **1999**, *9*, 59.
(67) Nakagawa, Y.; Zones, S. I. In *Synthesis of Microporous Materials*; Occelli, M. L., Robson, H., Eds.; Van Nostrand Reinhold: New York, 1992; Vol. 1, pp 222−239.
(68) Villaescusa, L. A.; Barrett, P. A.; Camblor, M. A. *Chem. Mater.* **1998**, *10*, 3966.
(69) Diaz-Cabañas, M. J.; Barrett, P. A.; Camblor, M. A. *Chem. Commun.* **1998**, 1881.
(70) Shantz, D. F.; Burton, A.; Lobo, R. F. *Microporous Mesoporous Mater.* **1999**, *31*, 61.
(71) Blasco, T.; Corma, A.; Diaz-Cabañas, M. J.; Rey, F.; Vidal-Moya, J. A.; Zicovich-Wilson, C. M. *J. Phys. Chem. B* **2002**, *106*, 2634.